PHYSICAL REVIEW B **96**, 020507(R) (2017)

Controlling topological superconductivity by magnetization dynamics

Vardan Kaladzhyan,[1,2,*] Pascal Simon,[2,†] and Mircea Trif[3,‡]

[1]*Institut de Physique Théorique, CEA/Saclay, Orme des Merisiers, 91190 Gif-sur-Yvette Cedex, France*

[2]*Laboratoire de Physique des Solides, CNRS, Université Paris-Sud, Université Paris-Saclay, 91405 Orsay Cedex, France*

[3]*Institute for Interdisciplinary Information Sciences, Tsinghua University, Beijing, China*

(Received 10 March 2017; published 28 July 2017)

We study theoretically a chain of precessing classical magnetic impurities in an s-wave superconductor. Utilizing a rotating wave description, we derive an effective Hamiltonian that describes the emergent Shiba band. We find that this Hamiltonian shows nontrivial topological properties, and we obtain the corresponding topological phase diagrams both numerically and analytically. We show that changing precession frequency offers control over topological phase transitions and the emergence of Majorana bound states. We propose driving the magnetic impurities or magnetic texture into precession by means of spin-transfer torque in a spin Hall setup, and manipulate it using spin superfluidity in the case of planar magnetic order.

DOI: 10.1103/PhysRevB.96.020507

Introduction. The search for topological phases of matter during the last decade has led to remarkable advancements in engineering systems with preassigned exotic excitations such as the Dirac, Weyl, or Majorana fermions. The latter have been pursued in numerous condensed matter setups [1], as they have been suggested as promising candidates for fault-tolerant topological quantum computing [2].

Ubiquitous and destructive by its nature for other phenomena, disorder has become one of the most interesting and reliable tools to build the sought-for topological systems. Discovered more than half a century ago [3–6], impurity-induced bound states in superconductors have been recently brought to life in the experiments [7,8]. The latter, along with the rise of topological phases of matter, initiated a series of works, both theoretical [9–26] and experimental [27–30], proposing to use Shiba states as promising building blocks for desired Majorana-supporting systems. The underlying mechanism is reminiscent of that of electronic bands appearing in solids: Being brought together, discrete Shiba levels originating from different impurities hybridize and form Shiba bands, with electrons filling them according to the Pauli principle. The resulting band structure corresponds to that of a p-wave, or topological, superconductor that can exhibit Majorana edge modes depending on the parameters of the system under consideration. The drawback of such an implementation, however, is that system parameters are typically fixed, and one cannot explore easily the full phase diagram.

In this Rapid Communication, motivated by recent progress in the so-called dynamical, or Floquet topological, insulators [31,32], we present a promising setup not only for engineering a topological superconducting phase, but most remarkably for *controlling* the topological phase transition by means of magnetization texture dynamics. We consider theoretically a "dynamical Shiba chain", that pertains to a set of classical magnetic impurities with precessing spins deposited on top of a two-dimensional (2D) s-wave superconductor (see Fig. 1). We find that such a dynamical magnetic texture can give rise

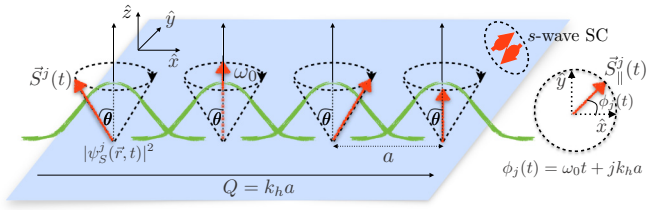

FIG. 1. Sketch of the precessing spin helix in a two-dimensional s-wave superconductor (the blue plane). The classical spins (red arrows) are separated by a distance a and precess around the z axis with a frequency ω_0 at a polar angle θ. The precession azimuthal angle $\phi_j(t) = \omega_0 t + k_h j a$, with k_h the step of the helix and j the position of the spin in the chain. The local dynamical Shiba state wave functions which overlap to eventually give a dynamical Shiba band are shown in green.

to a nontrivial Shiba band which can be controlled by tuning the precession frequency. Such features are different from previous time-dependent Floquet superconducting systems (see, for example, Refs. [33]), in that the band is not manipulated directly by external fields, but indirectly, by the dynamics of the magnetic texture that stirs the superconductor underneath and causes the appearance of such a band. This is inherently a strong coupling regime, as the magnetic texture is the reason for such a band to occur in the first place.

Model. The Hamiltonian describing our dynamical systems reads [10]

$$H_{\rm tot}(t) = H_0 + H_{\rm imp}(t), \tag{1}$$

where

$$H_0 = \xi_k \tau_z + \Delta_s \tau_x, \tag{2}$$

$$H_{\rm imp}(t) = J \sum_j \boldsymbol{S}^j(t) \cdot \boldsymbol{\sigma}\, \delta(\boldsymbol{r} - \boldsymbol{r}_j) \tag{3}$$

are the sum of the Bogoliubov–de Gennes Hamiltonian for the superconductor and its coupling to the magnetic impurities, respectively. Here, H_0 is written in the Nambu basis $\{c_{\boldsymbol{k}\uparrow}, c_{\boldsymbol{k}\downarrow}, c^\dagger_{-\boldsymbol{k}\downarrow}, -c^\dagger_{-\boldsymbol{k}\uparrow}\}^{\rm T}$, with $\boldsymbol{\sigma} = (\sigma_x, \sigma_y, \sigma_z)$ and $\boldsymbol{\tau} = (\tau_x, \tau_y, \tau_z)$ matrices acting in spin and particle-hole sub-

*vardan.kaladzhyan@cea.fr
†pascal.simon@u-psud.fr
‡trif@mail.tsinghua.edu.cn

spaces, respectively. The superconducting order parameter is denoted by Δ_s, and the spectrum of free electrons is defined as $\xi_k \equiv k^2/2m - \varepsilon_F$, where ε_F is the Fermi energy, and J is the exchange coupling between the spins and the electrons in the superconductor. Below, we also set $\hbar$ to unity. For the periodically driven magnetic chain we assume that the impurities are localized at positions $\boldsymbol{r}_j$, and have precessing spins that are defined as $\boldsymbol{S}^j(t) \equiv [\sin\theta\cos(\omega_0 t + \phi_j), \sin\theta\sin(\omega_0 t + \phi_j), \cos\theta]$, with precession frequency ω_0, polar angle θ as shown in Fig. 1, and equidistant individual phase shifts $\phi_j \equiv k_h a j$, $j \in \mathbb{Z}$. In the latter, a denotes the spacing between impurities, and k_h is the so-called helix step.

The time-dependent Schrödinger equation reads $i\partial_t \Psi(\boldsymbol{r},t) = H_{\rm tot}\Psi(\boldsymbol{r},t)$. This Hamiltonian is periodic, $H_{\rm tot}(t+T) = H_{\rm tot}(t)$, with $T = 2\pi/\omega_0$ and, moreover, the symmetry of the problem allows us to perform a time-dependent unitary transformation that makes the problem fully static. We can write $\Psi(\boldsymbol{r},t) = U(t)\Phi(\boldsymbol{r})e^{-iEt}$, with $U(t) = e^{-i\omega_0 t\sigma_z/2}$, so that we obtain the stationary Schrödinger equation

$$\mathcal{H}_F\Phi(\boldsymbol{r}) = E\Phi(\boldsymbol{r}), \tag{4}$$

where $\mathcal{H}_F \equiv H_{\rm tot}(0) - B\sigma_z$. Here, $B \equiv \omega_0/2$ is a fictitious magnetic field perpendicular to the plane of the superconductor, which will be referred to as the "driving frequency" hereinafter, and E is the quasienergy defined modulo $\omega_0/2$. Now, let us make a more concise connection with the usual stroboscopic, or Floquet, description of periodically driven systems. The full evolution operator for the driven chain can be written as

$$U_{\rm tot}(t) = e^{-iB\sigma_z t}e^{-i\mathcal{H}_F t}. \tag{5}$$

After one period T, the evolution operator can be written $U_{\rm tot}(T) = \exp(-i\mathcal{H}_F T)$ (up to a sign), with $\mathcal{H}_F$ identifying as the Floquet Hamiltonian describing the evolution of the system at $t = nT$, with $n \in \mathbb{N}$ (stroboscopically). The Hamiltonian $\mathcal{H}_F$ gives rise to a quasienergy spectrum defined up to integer multiples of $2B$ and, as in the static case, can result in nontrivial topological properties which in an open system are identified with the appearance of edge states. However, it does not fully characterize the topological structure and the entire spectrum of edge states of the driven system. Such a complete description was developed recently in several works, where they showed that in order to fully describe that, one needs the evolution operator at all times t, not only at $t = T$. However, for our situation of circular spin texture precession, it turns out that $\mathcal{H}_F$ describes fully the topological structure of the driven system, and thus we focus on that aspect only in the following.

As discussed in Ref. [34], a single magnetic impurity with a periodically driven spin gives rise to a pair of Shiba states residing in the effective gap $\Delta_s^{\rm eff} = \Delta_s - B$, provided the driving frequency B is smaller than the superconducting gap Δ_s. This condition is essential to have a gapful system and well-defined impurity-induced subgap states. The energies of these states in the deep-dilute regime ($\alpha \sim 1$) are given by $\pm\epsilon_0(B)$, where

$$\epsilon_0(B) \equiv \left[\left(1 - \frac{1}{\alpha}\right)\Delta_s - B\cos\theta\right], \tag{6}$$

and $\alpha \equiv \pi\nu_0 J$ is the dimensionless impurity strength parameter written in terms of normal-phase density of states ν_0. It has been shown in Refs. [13,14] that a static helical chain of magnetic impurities produces a 4×4 Shiba band structure with nontrivial topological properties. Moreover, for $\alpha \approx 1$, one can project the resulting 4×4 Hamiltonian onto an effective 2×2 that fully characterizes the low-energy spectrum (the energy separation between the bands is of order Δ_s).

Hereafter we use Eq. (4) and, following the procedure described in Ref. [13], we derive the effective 2×2 Hamiltonian for the emerging Shiba band. The details of this derivation are given in the Supplemental Material (SM) [35].

Effective band structure. The effective Hamiltonian describing the Shiba band in the rotating frame in both aforementioned cases can be written by exploiting the $\boldsymbol{d}$-vector notation as

$$\mathcal{H}_{\rm S}(k) = d_0(k) + \boldsymbol{d}(k)\cdot\boldsymbol{\Sigma}, \tag{7}$$

with

$$\begin{aligned} d_0(k) &= [\Delta_s\cos\theta - B(1-\alpha\sin^2\theta)]F_0(B,ka,k_Fa),\\ d_x(k) &= (\Delta_s - \alpha B\cos\theta)F_x(B,ka,k_Fa)\sin\theta,\\ d_z(k) &= -\epsilon_0(B) + (\Delta_s - B\cos\theta)F_z(B,ka,k_Fa), \end{aligned} \tag{8}$$

and $d_y(k) \equiv 0$. Equations (8) represent one of our main results. Here, $\boldsymbol{\Sigma} = (\Sigma_x,\Sigma_y,\Sigma_z)$ represents a resulting Nambu space which, however, is a complicated admixture of $\boldsymbol{\sigma}$ and $\boldsymbol{\tau}$. The form of the functions $F_{0,x,z}(B,ka,k_Fa)$ is in general too complicated to be displayed. However, there are various limiting cases where analytical progress is possible. In this Rapid Communication we focus on two limiting cases that can be studied both analytically and numerically, i.e., the short and the long coherence length, respectively. The first case corresponds to a chain with only nearest-neighbor hopping, in other words, the case of a small coherence length $\xi \ll a$, where $\xi \equiv v_F/\sqrt{\Delta_s^2 - B^2}$. In this limit, we need to set in Eq. (8) the following functions,

$$\begin{aligned} F_{0,x}(B,ka,k_Fa) &\equiv \tilde{X}_{0,1}(a)\sin\frac{k_h a}{2}\sin ka,\\ F_z(B,ka,k_Fa) &\equiv \tilde{X}_0(a)\cos\frac{k_h a}{2}\cos ka, \end{aligned} \tag{9}$$

where

$$\tilde{X}_{0(1)}(a) = -\frac{2}{\pi}\,{\rm Im(Re)}\,{\rm K}_0\left[-i\left(1 + i\frac{1}{k_F\xi}\right)k_Fa\right],$$

with k_F being the Fermi momentum and $\rm K_0$ denoting the zeroth modified Bessel function of the second kind (for further details, see Ref. [35] as well as Ref. [36]). Note that the functions $\tilde{X}_{0,1}$ depend at least quadratically on the fictitious magnetic field B, and for $B \ll \Delta_s$ we can neglect such dependence in leading order.

The second limiting case describes a chain with very extended Shiba states, i.e., with a large coherence length compared to the impurity spacing, $\xi \gg a$. Contrary to the small coherence length regime, here all the higher-order hopping processes become possible. In this regime we obtain the following expressions for the functions $F_{0,x,z}$ in Eq. (7), $F_{0,x} \equiv [F_{0,1}^-(k) - F_{0,1}^+(k)]/2$ and $F_z \equiv [F_0^-(k) + F_0^+(k)]/2$,

where we defined

$$F^{s}_{0(1)}(k) \equiv \sqrt{\frac{2}{\pi k_F a}}\,\mathrm{Im(Re)}\, f_s(k),$$

with $s = \pm$ and

$$f_s(k) = e^{-i\frac{\pi}{4}}\left[\mathrm{Li}_{\frac{1}{2}}(e^{i(k+sk_h/2-k_F)a}) + \mathrm{Li}_{\frac{1}{2}}(e^{-i(k+sk_h/2+k_F)a})\right], \tag{10}$$

expressed in terms of the polylogarithm function $\mathrm{Li}(x)$.

Note that $d_x(k)$ in the expressions given above plays the role of the gap parameter Δ_k from Ref. [13], which, in the limit of $B \ll \Delta_s$, is only slightly reduced by the fictitious field. On the other hand, $d_z(k)$ is strongly affected by the driving, as it results in a shift of the alignment of the Shiba bands, and eventually their topology. While $d_0(k)$ does not change the topology of the bands, it does affect their overlap (the absolute gap), and it can also depend strongly on B for $\theta \to \pi/2$ (planar helix). In fact, in such a case, the entire dependence on the magnetic field arises through this term in leading order which, however, is small for $\alpha \sim 1$.

Quasispectrum and topology. In what follows, we study the topological properties of the Hamiltonian in Eq. (7) in the short and long coherence length regimes introduced above. The spectrum can be found easily as $E(k) = d_0(k) \pm \sqrt{d_z^2(k) + d_x^2(k)}$, which, because of the periodic drive, is uniquely defined only up to an integer multiple of B. Thus, we need to fold the resulting spectrum into the first quasienergy Brillouin zone, $E(k) \in [-B, B)$. The resulting one-dimensional Hamiltonian is real, and thus it belongs to the BDI symmetry class [37]. In this case the number of Majorana states emerging at one end in the case of open boundary conditions is given not by a $\mathbb{Z}_2$, but by a $\mathbb{Z}$ invariant [38], which reads

$$\mathcal{W} = \frac{1}{2\pi}\int_{-\pi}^{\pi} d\theta(k), \tag{11}$$

with $\theta(k) = \mathrm{Arg}[d_x(k) + i d_z(k)]$. This winding number characterizes the number of edge states. However, it does not indicate the presence of an absolute gap in the system, meaning that it can be well defined even if the system is gapless. We depict such surprising features in Fig. 2, where we plot the absolute gap between the Shiba bands, as well as the corresponding winding number, as functions of the driving frequency B against the Fermi momentum k_F (angle θ) in the left (right) column. Both the driving frequency and the precession angles are tunable parameters and, most strikingly, this shows that the system can undergo a topological phase transition by changing the driving frequency.

We note that for the small coherence length regime (top row) the winding number can be calculated analytically (see Ref. [35]), whereas for the large coherence length (bottom row) we restrict ourselves to computing the integral in Eq. (11) only numerically [39]. A few more comments are in order. As expected for $\theta = 0$ (corresponding to a ferromagnetic arrangement of the impurity spins), the gap is absent and the system is in a gapless trivial phase with zero winding number. Conversely, when $\theta = \pi/2$, the spin helix is planar. This in turn means that the fictitious magnetic field B appearing in the rotating frame [see Eq. (4)] does not couple to the chain, which

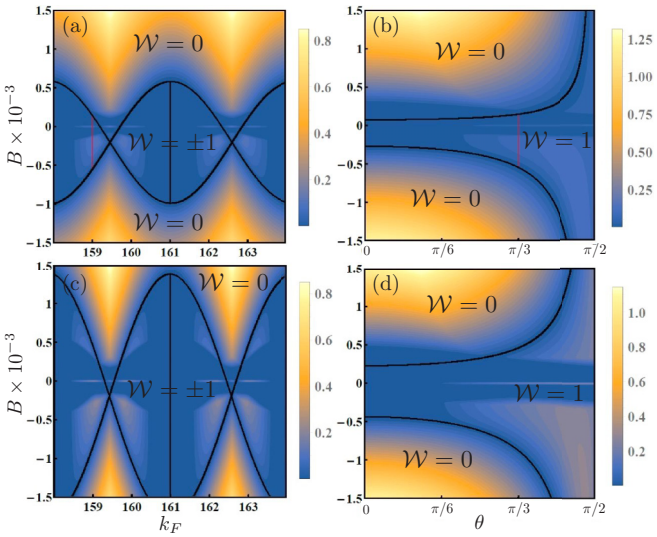

FIG. 2. The gap around quasienergy $E = 0$ and the winding number of the Shiba band for the small and large coherence length regimes (first and second rows, respectively), plotted as functions of the driving frequency B and the Fermi momentum k_F (precession angle θ) in the left (right) column. The continuous black lines separate regions with different winding numbers $\mathcal{W}$ which are well defined even for the gapless regions. The vertical red lines highlight the existence of localized Majorana end states in an open system (see Fig. 3 for details). We set $k_h = \pi/4$, $v_F = 0.2$, $\Delta_s = 1$, $a = 1$, $\alpha = 0.9999$. The polar angle $\theta = \pi/3$ and $k_F = 159$ in the left and right columns correspondingly.

explains why no change of phase occurs while changing the driving frequency for $\theta = \pi/2$. Therefore, the system always enters a topological superconducting phase.

One of the most important signatures of topological systems are topological edge states. In Fig. 3 we show the quasispectrum for a dynamical chain with open boundary conditions and for the case of a short coherence length. We see that Majorana bound states (MBS) emerge at zero energy (red line), and that their existence range is in perfect agreement with the bulk winding number calculation. Moreover, we found that the MBS even exist in regions where the system is gapless, albeit they are no longer protected by the gap and any impurities could easily mix them with the bulk (extended) states. By changing the driving frequency of the precessing spins, we demonstrate that our setup enters one of the four following phases: trivial, gapless or gapful, or topological, gapless or gapful, thus covering all the possibilities. While for a region of the parameter space we found gaps at both $E = 0$ and $E = B$ (see Fig. 3), only the modes at the former are emerging for the circular driving utilized here. However, such a conclusion should not hold for more general drivings of the magnetic texture.

Detection and physical implementations. The dynamically generated MBS described above could be detected in transport measurements by a nearby voltage-biased scanning tunneling microscopy (STM) tip [40]. Alternatively, one could utilize a recent scheme that relies on the pumped charge by the precessing texture into the STM tip at different positions in the chain in the absence of any applied voltage [34,41]. In order to

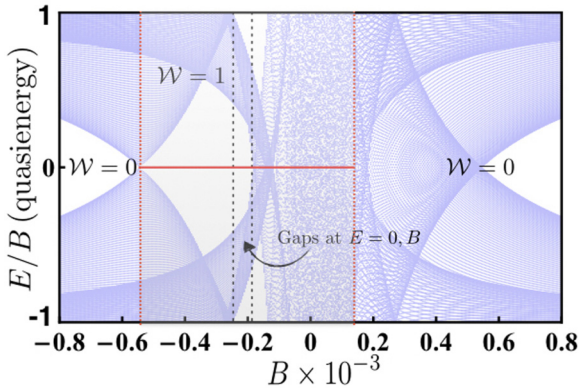

FIG. 3. The quasispectrum (normalized by the driving B) for an open Shiba chain, in the regime of small coherence length as a function of the driving frequency B. The horizontal red line stands for the zero quasienergy Majorana end mode, while $\mathcal{W}$ defines the bulk winding number (see main text). A region with two gaps, at $E=0$ and $E=B$, exists, but the latter is trivial as we find no Majoranas emerging. We set $k_F=159$, $k_h=\pi/4$, $v_F=0.2$, $\Delta_s=1$, $a=1$, $\theta=\pi/3$, $\alpha=0.9999$.

generate the dynamics, we envision several implementations, depending on the way the magnetic texture emerges in the first place. In the case of a preformed helix, either due to the Ruderman-Kittel-Kasuya-Yosida (RKKY) interaction mediated by electrons in the superconductor [12], or due to the spin-orbit interaction (SOI) in the substrate [42], the precession of the helix corresponds simply to global rotations. The traditional way to excite such a mode is by driving the helix with microwaves that excite the ferromagnetic resonance associated with such a rotation mode. However, in recent years there has been tremendous progress in exciting magnetic devices in transport setups by means of the spin Hall effect [43]. Such a setup would allow for an all-electrical implementation of a dynamical magnetic texture–superconductor hybrid, with a controllable frequency (see Ref. [35] for details on the implementation). Both these methods can give rise to rotations of the helix, but do not result in changes of the pitch. However, when the impurities form a planar ferromagnet (with the exchange interaction keeping the spins in a plane), it becomes possible to control the pitch k_h, the frequency ω, and the cone angle θ by means of spin biases, as showed recently in several works [44]. This goes by the name of spin superfluidity, as there is a direct mapping between a superfluid flow (such as in He_4) and the magnetization flow in such a planar spin configuration. As detailed in Ref. [35], such manipulations are possible simply by changing the spin biases induced by the spin Hall effect applied over the planar spin configuration, with a pitch in one-to-one correspondence with the spin supercurrent flowing through the magnetic system, and an adjustable frequency depending on the relative biases [44].

Discussions and perspectives. The setup proposed in this Rapid Communication can be generalized to a chain of precessing magnetic impurities deposited on top of a three-dimensional (3D) superconductor. Despite a modification in the Shiba wave-function coherence length, we expect no qualitative difference in our main argument concerning a controlled topological phase transition. Moreover, a 3D superconductor is expected to reflect the short coherence length regime, whereas a 2D one can reflect the long coherence length regime. As a future extension of this work we propose to consider more complicated networks of driven magnetic impurities, e.g., a 2D array. Also, generalizations to more complicated textures and precessions is in order, as our perfect rotation wave description would break down, and a fully Floquet approach would be required. The same arguments should apply when the substrate (superconductor) possesses a spin-orbit interaction.

In conclusion, here we proposed a way to engineer a controllable topological phase transition by means of magnetization texture dynamics. We have shown that a chain of precessing classical spins deposited on top of an s-wave superconductor gives rise to a topologically nontrivial Shiba band, and we have demonstrated that topological phase transitions in such a band can be controlled by changing the driving frequency, a tunable parameter in the spin transport experiments.

Acknowledgments. We would like to thank Cristina Bena, So Takei, and Yaroslav Tserkovnyak for useful discussions. P.S. would like to acknowledge financial support from the French Agence Nationale de la Recherche through the contract ANR Mistral. M.T. would like to acknowledge financial support from the National Basic Research Program of China Grants No. 2011CBA00300 and No. 2011CBA00302.

[1] See the review article by S. D. Sarma, M. Freedman, and C. Nayak, npj Quantum Inf. **1**, 15001 (2015).
[2] A. Kitaev, Ann. Phys. **303**, 2 (2003).
[3] L. Yu, Acta Phys. Sin. **21**, 75 (1965).
[4] H. Shiba, Prog. Theor. Phys. **40**, 435 (1968).
[5] A. I. Rusinov, Sov. J. Exp. Theor. Phys. Lett. **9**, 85 (1969).
[6] A. Sakurai, Prog. Theor. Phys. **44**, 1472 (1970).
[7] A. Yazdani, B. A. Jones, C. P. Lutz, M. F. Crommie, and D. M. Eigler, Science **275**, 1767 (1997).
[8] G. Ménard *et al.*, Nat. Phys. **11**, 1013 (2015).
[9] T.-P. Choy, J. M. Edge, A. R. Akhmerov, and C. W. J. Beenakker, Phys. Rev. B **84**, 195442 (2011).
[10] S. Nadj-Perge, I. K. Drozdov, B. A. Bernevig, and A. Yazdani, Phys. Rev. B **88**, 020407 (2013).
[11] S. Nakosai, Y. Tanaka, and N. Nagaosa, Phys. Rev. B **88**, 180503 (2013).
[12] B. Braunecker and P. Simon, Phys. Rev. Lett. **111**, 147202 (2013); J. Klinovaja, P. Stano, A. Yazdani, and D. Loss, *ibid.* **111**, 186805 (2013); M. M. Vazifeh and M. Franz, *ibid.* **111**, 206802 (2013); M. Schecter, K. Flensberg, M. H. Christensen, B. M. Andersen, and J. Paaske, Phys. Rev. B **93**, 140503 (2016); M. H. Christensen, M. Schecter, K. Flensberg, B. M. Andersen, and J. Paaske, *ibid.* **94**, 144509 (2016).
[13] F. Pientka, L. I. Glazman, and F. von Oppen, Phys. Rev. B **88**, 155420 (2013).

[14] F. Pientka, L. I. Glazman, and F. von Oppen, Phys. Rev. B **89**, 180505 (2014).
[15] K. Pöyhönen, A. Weststrom, J. Röntynen, and T. Ojanen, Phys. Rev. B **89**, 115109 (2014).
[16] A. Heimes, P. Kotetes, and G. Schön, Phys. Rev. B **90**, 060507 (2014).
[17] A. Weststrom, K. Pöyhönen, and T. Ojanen, Phys. Rev. B **91**, 064502 (2015).
[18] J. Röntynen and T. Ojanen, Phys. Rev. Lett. **114**, 236803 (2015).
[19] P. M. R. Brydon, S. Das Sarma, H.-Y. Hui, and J. D. Sau, Phys. Rev. B **91**, 064505 (2015).
[20] Y. Peng, F. Pientka, L. I. Glazman, and F. von Oppen, Phys. Rev. Lett. **114**, 106801 (2015).
[21] B. Braunecker and P. Simon, Phys. Rev. B **92**, 241410 (2015).
[22] J. Zhang, Y. Kim, E. Rossi, and R. M. Lutchyn, Phys. Rev. B **93**, 024507 (2016).
[23] S. Hoffman, J. Klinovaja, and D. Loss, Phys. Rev. B **93**, 165418 (2016).
[24] T. Neupert, A. Yazdani, and B. A. Bernevig, Phys. Rev. B **93**, 094508 (2016).
[25] L. Kimme and T. Hyart, Phys. Rev. B **93**, 035134 (2016).
[26] V. Kaladzhyan, J. Röntynen, P. Simon, and T. Ojanen, Phys. Rev. B **94**, 060505 (2016).
[27] S. Nadj-Perge, I. K. Drozdov, J. Li, H. Chen, S. Jeon, J. Seo, A. H. MacDonald, B. A. Bernevig, and A. Yazdani, Science **346**, 602 (2014).
[28] M. Ruby, F. Pientka, Y. Peng, F. von Oppen, B. W. Heinrich, and K. J. Franke, Phys. Rev. Lett. **115**, 197204 (2015).
[29] R. Pawlak, M. Lisiel, J. Klinovaja, T. Meier, S. Kawai, T. Gladzel, D. Loss, and E. Meyer, npj Quantum Inf. **2**, 16035 (2016).
[30] B. E. Feldman *et al.*, Nat. Phys. **13**, 286 (2017).
[31] T. Kitagawa, E. Berg, M. Rudner, and E. Demler, Phys. Rev. B **82**, 235114 (2010).
[32] N. H. Lindner, G. Refael, and V. Galitski, Nat. Phys. **7**, 490 (2011).
[33] L. Jiang, T. Kitagawa, J. Alicea, A. R. Akhmerov, D. Pekker, G. Refael, J. I. Cirac, E. Demler, M. D. Lukin, and P. Zoller, Phys. Rev. Lett. **106**, 220402 (2011); M. Trif and Y. Tserkovnyak, *ibid.* **109**, 257002 (2012); Q.-J. Tong, J.-H. An, J. Gong, H.-G. Luo, and C. H. Oh, Phys. Rev. B **87**, 201109 (2013); M. Thakurathi, A. A. Patel, D. Sen, and A. Dutta, *ibid.* **88**, 155133 (2013); A. Gómez-León and G. Platero, Phys. Rev. Lett. **110**, 200403 (2013); D. E. Liu, A. Levchenko, and H. U. Baranger, *ibid.* **111**, 047002 (2013); A. Poudel, G. Ortiz, and L. Viola, Europhys. Lett. **110**, 17004 (2015); J. Klinovaja, P. Stano, and D. Loss, Phys. Rev. Lett. **116**, 176401 (2016).
[34] V. Kaladzhyan, S. Hoffman, and M. Trif, Phys. Rev. B **95**, 195403 (2017).
[35] See Supplemental Material at http://link.aps.org/supplemental/10.1103/PhysRevB.96.020507 for derivation of the effective Hamiltonian in Eqs. (7)–(8), generalization to a spin-orbit coupled system, as well as a description of the proposed experimental implementation of the dynamical setup.
[36] V. Kaladzhyan, C. Bena, and P. Simon, J. Phys.: Condens. Matter **28**, 485701 (2016).
[37] A. P. Schnyder, S. Ryu, A. Furusaki, and A. W. W. Ludwig, Phys. Rev. B **78**, 195125 (2008).
[38] S. Tewari and J. D. Sau, Phys. Rev. Lett. **109**, 150408 (2012).
[39] It is worth mentioning that the topologically nontrivial regions in Fig. 2 can be also determined by utilizing Pfaffian invariants reflecting parity of the winding number $\mathcal{W}$, as well as by employing the so-called "singular points technique" developed in Ref. [45].
[40] A. Kundu and B. Seradjeh, Phys. Rev. Lett. **111**, 136402 (2013).
[41] M. Trif, V. Kaladzhyan, and P. Simon (unpublished).
[42] J. Li, T. Neupert, B. A. Bernevig, and A. Yazdani, Nat. Commun. **7**, 10395EP (2016).
[43] J. Sinova, S. O. Valenzuela, J. Wunderlich, C. H. Back, and T. Jungwirth, Rev. Mod. Phys. **87**, 1213 (2015).
[44] J. König, M. C. Bønsager, and A. H. MacDonald, Phys. Rev. Lett. **87**, 187202 (2001); E. Sonin, Adv. Phys. **59**, 181 (2010); S. Takei and Y. Tserkovnyak, Phys. Rev. Lett. **112**, 227201 (2014).
[45] V. Kaladzhyan, J. Despres, I. Mandal, and C. Bena, arXiv:1611.09367.